



## Effect of tetragonal distortion on ferroelectric domain switching: A case study on La-doped BiFeO<sub>3</sub> – PbTiO<sub>3</sub> ceramics

Thorsten Leist, Torsten Granzow, Wook Jo, and Jürgen Rödel

Citation: *Journal of Applied Physics* **108**, 014103 (2010); doi: 10.1063/1.3445771

View online: <http://dx.doi.org/10.1063/1.3445771>

View Table of Contents: <http://scitation.aip.org/content/aip/journal/jap/108/1?ver=pdfcov>

Published by the [AIP Publishing](#)

---

### Articles you may be interested in

Domain switching energies: Mechanical versus electrical loading in La-doped bismuth ferrite–lead titanate  
*J. Appl. Phys.* **109**, 054109 (2011); 10.1063/1.3555599

High-throughput evaluation of domain switching in piezoelectric ceramics and application to Pb Zr<sub>0.6</sub> Ti<sub>0.4</sub> O<sub>3</sub> doped with La and Fe  
*Appl. Phys. Lett.* **93**, 152904 (2008); 10.1063/1.2999623

Physical mechanism for orientation dependence of ferroelectric fatigue in Pb ( Zn<sub>1/3</sub> Nb<sub>2/3</sub> ) O<sub>3</sub> 5 % PbTiO<sub>3</sub> crystals  
*J. Appl. Phys.* **96**, 7471 (2004); 10.1063/1.1812815

Polarization switching in (001)-oriented Pb ( Mg<sub>1/3</sub> Nb<sub>2/3</sub> ) O<sub>3</sub> – x % PbTiO<sub>3</sub> crystals: Direct observation of heterogeneous nucleation by piezoreponse force microscopy  
*Appl. Phys. Lett.* **85**, 4457 (2004); 10.1063/1.1819993

Effect of Pb(Yb<sub>1/2</sub> Nb<sub>1/2</sub> )O<sub>3</sub> on structural and piezoelectric properties of Pb(Zr<sub>0.52</sub> Ti<sub>0.48</sub> )O<sub>3</sub> ceramics  
*J. Appl. Phys.* **88**, 3596 (2000); 10.1063/1.1288222

---

A banner for the 2014 Special Topics section. The background is a dark orange gradient. At the top center, the text '2014 Special Topics' is written in a large, white, sans-serif font. Below this text, five circular icons are arranged horizontally, each containing a different material-related image and a label. From left to right: 1. A red and black molecular structure labeled 'PEROVSKITES'. 2. A blue and red atomic lattice labeled '2D MATERIALS'. 3. A green and black porous structure labeled 'MESOPOROUS MATERIALS'. 4. A yellow and black microscopic image labeled 'BIOMATERIALS/ BIOELECTRONICS'. 5. A brown and black porous structure labeled 'METAL-ORGANIC FRAMEWORK MATERIALS'. At the bottom left, the 'AIP | APL Materials' logo is displayed. At the bottom right, a red ribbon contains the text 'Submit Today!' in white.

# Effect of tetragonal distortion on ferroelectric domain switching: A case study on La-doped BiFeO<sub>3</sub>–PbTiO<sub>3</sub> ceramics

Thorsten Leist,<sup>a)</sup> Torsten Granzow, Wook Jo, and Jürgen Rödel  
*Institute of Materials Science, Technische Universität Darmstadt, 64287 Darmstadt, Germany*

(Received 11 December 2009; accepted 9 May 2010; published online 6 July 2010)

The ferroelectric and piezoelectric properties of  $(1-x)\text{BiFeO}_3-x\text{PbTiO}_3$  (BF-PT) ceramics were investigated as a function of tetragonal distortion. The latter was adjusted by employing La-doping (0–30 at %) while keeping the material near the morphotropic phase boundary by varying  $x$  between 0.35 and 0.46. This allows changing the  $c/a$  ratio of tetragonal BF-PT in the range from 1.10–1.01 and consequently alters the level of compatibility stresses. It was found that the  $c/a$  ratio has a significant influence on domain switching as inferred from electric field induced polarization, strain hysteresis, and Rayleigh measurements. Specifically, a threshold  $c/a$  ratio of about 1.045 was identified below which the electric field induced domain mobility increases sharply.

© 2010 American Institute of Physics. [doi:10.1063/1.3445771]

## I. INTRODUCTION

Piezoelectric actuators and sensors based on ferroelectrics with perovskite structure have found their way into many applications due to their excellent properties. Both during poling as well as during electric field-induced actuation, domain switching is of paramount importance. Electrical as well as mechanical driving forces influence domain switching. A macroscopic mechanical stress can either hamper or alleviate the switching behavior of ferroelectrics,<sup>1–4</sup> depending on the relative orientation of compressive stress and electric field. For example, Lynch<sup>1</sup> showed that a compressive stress applied parallel to the poling direction can almost completely suppress domain switching in ferroelectrics. Similarly, ferroelectric thin films experience compatibility stresses, which have been introduced due to a lattice mismatch between substrate and ferroelectric coating. This again affects the switching behavior of the ferroelectric.<sup>5,6</sup> On a microstructural level, internal stresses are also believed to cause depolarization, as observed in PZT below the Curie temperature.<sup>7</sup>

In ferroelectrics, internal stresses are introduced by cooling down from the paraelectric cubic phase into the ferroelectric tetragonal phase. In pure polycrystalline PbTiO<sub>3</sub> (PT),  $c/a$  ratio of 1.06 leads to internal mechanical stresses large enough to disintegrate the ceramic.<sup>8</sup>  $(1-x)\text{BiFeO}_3-x\text{PbTiO}_3$  (BF-PT), a high temperature piezoelectric,<sup>9–13</sup> is expected to contain even higher internal misfit strains as its  $c/a$  ratio lies at 1.10 for  $x=0.35$  after sintering.<sup>13</sup> Hence, it is apparent that the  $c/a$  ratio provides local misfit strains and is connected through the elasticity tensor to internal stresses. However, experimental studies on the effect of tetragonal distortion, i.e.,  $c/a$  ratio, on the switching behavior of ferroelectrics are not available. Specifically, knowledge of optimum tetragonal distortions for

poling and electric-field induced actuation could guide development of new piezoelectric ceramics, e.g., lead-free or high-temperature piezoceramics.

La-doping has been shown to reduce the  $c/a$  ratio of BF-PT from 1.10 down to 1.01.<sup>14–18</sup> Therefore, BF-PT with eight different La-contents was utilized as a model system to study the influence of  $c/a$  ratio on the domain switching behavior of ferroelectrics. As domain switching is affected by the distance to the respective morphotropic phase boundary (MPB), the BF/PT ratio was readjusted to the altered La-content to assure that all materials are at an MPB.

## II. EXPERIMENTAL PROCEDURE

La-doped solid solutions of BF-PT with the formula  $(1-x)(\text{Bi}_{1-y}\text{La}_y)\text{FeO}_3-x\text{PbTiO}_3$  were prepared by the conventional solid oxide processing route. Based on our preliminary studies,<sup>19</sup>  $x$  was chosen as 0.35, 0.39, 0.40, 0.41, 0.415, 0.43, 0.44, and 0.46 for each  $y$  value of 0, 0.025, 0.05, 0.075, 0.1, 0.15, 0.2, and 0.3, respectively, to ensure that each system is mixed phase. The aim was to keep the fraction of rhombohedral and tetragonal phase as close to 50% as possible. However, as shown in earlier publications, even significant deviations from this ratio in  $(1-x)(\text{Bi}_{1-y}\text{La}_y)\text{FeO}_3-x\text{PbTiO}_3$  were found to have only little influence on the material properties.<sup>19</sup> In the following, the acronym BF-PT will always refer to one or more of the particular compositions used in our experiments. An overview of the composition of our samples is also given in Table I.

Precursor oxides of Bi<sub>2</sub>O<sub>3</sub>, La<sub>2</sub>O<sub>3</sub>, Fe<sub>2</sub>O<sub>3</sub>, TiO<sub>2</sub>, and PbO (purity  $\geq 99.5\%$ , AlfaAesar) were weighed according to the stoichiometric formula and homogeneously mixed in a planetary ball mill for 1 h at 180 rpm. Calcination of the powder mixture was performed at 800 °C for 5 h. After calcination a second milling step in a planetary ball mill was carried out at 180 rpm for 24 h to ensure fine grained and uniform powders. Compacted pellets of 10 mm in diameter with a thickness of about 1 mm were hydrostatically pressed at 350 MPa. Sintering of the pellets was performed at 925–1025 °C for 4

<sup>a)</sup>Author to whom correspondence should be addressed. Electronic mail: leist@ceramics.tu-darmstadt.de.

TABLE I. Compositional dependence of grain size, relative density, and Curie temperature ( $T_c$ ) for  $(1-x)(\text{Bi}_{1-y}\text{La}_y)\text{FeO}_3-x\text{PbTiO}_3$ .

$x\text{PbTiO}_3$	0.35	0.39	0.4	0.41	0.415	0.43	0.44	0.46
yLa	0	0.025	0.05	0.075	0.1	0.15	0.2	0.3
Grain size in ( $\mu\text{m}$ )	0.8 ( $\pm 0.21$ )	1.14 ( $\pm 0.24$ )	0.84 ( $\pm 0.24$ )	1.67 ( $\pm 0.2$ )	1.65 ( $\pm 0.21$ )	1.39 ( $\pm 0.34$ )	1.89 ( $\pm 0.39$ )	1.5 ( $\pm 0.29$ )
Relative density	96%	97%	94%	95%	95%	96%	95%	97%
$T_c$ <sup>a-c</sup>	632 °C	N.A.	N.A.	N.A.	386 °C	N.A.	264 °C	189 °C

<sup>a</sup>Reference 11.<sup>b</sup>Reference 14.<sup>c</sup>Reference 16.

h in a closed crucible depending on composition. The pellets were embedded in a powder bed of the same composition in order to minimize loss of volatile elements during sintering.

To remove a possible influence from polishing-induced residual stress during sample preparation,<sup>20</sup> all the ground and polished samples were thermally annealed at 650 °C for 12 min and subsequently cooled to room temperature using a cooling rate of 50 °C/h in order to avoid the creation of additional internal stresses. The  $c/a$  ratio of each composition was determined from x-ray diffraction (Bruker Siemens D5000) patterns of bulk specimens. A step size of 0.03° in a  $2\theta$  angular range from 10°–90° was employed with a measuring time of 5 s at each step. Diffraction patterns obtained from these samples were analyzed by a software package GSAS.<sup>21,22</sup> Lattice parameters obtained from the Rietveld refinement were used to calculate the theoretical density. Density measurements were conducted by using the Archimedes method. Grain size was measured by analyzing images from scanning electron microscopy (SEM, Philips XL 30 FEG, Eindhoven, The Netherlands) micrographs, using the line intersect software “LINCE” programmed by Sergio Luis dos Santos e Lucato (TU Darmstadt, FB Materials Science, Ceramics Group). For electrical characterization the sintered pellets were ground down to a thickness of 0.7 mm in order to remove the surface layer and electroded with silver paste. Field dependent polarization and strain were measured with a Sawyer–Tower circuit and an optical displacement sensor (Model D63-AI+H+LNPQ, Philtec). A triangular form of high voltage signal was applied to the sample with a high voltage amplifier (Trek Model 20/20C) that was driven by a function generator (Agilent 33220A). All experiments were carried out at a frequency of 4 Hz and with a maximum field of 8 kV/mm. Values of the piezoelectric coefficient  $d_{33}$  were determined after two unipolar cycles using a Berlincourt-meter (YE2730, Sinocera). Rayleigh analysis was conducted on unpoled samples by applying a sinusoidal ac-voltage signal to the sample and simultaneously recording the charges generated by the sample using a measurement capacitance and a lock-in amplifier (Model SR830 DSP). A computer was connected to the lock-in amplifier to collect the data. Frequencies of the voltage signal were set to 10 and 100 Hz with a maximum amplitude of 1.4 kV/mm.

### III. RESULTS

Table I displays the characteristic parameters of the microstructure of each sample. The grain size is slightly different for each La content, but there is no correlation between the two parameters. The density of all samples was between

94% and 97%. The table also shows the values of the Curie temperature of certain compositions that are known from the literature. Quantitative evaluation of the lattice parameters revealed both the tetragonal and rhombohedral distortions according to Uchida and Ikeda.<sup>23</sup> Figure 1 displays the monotonous change in  $c/a$  ratio from 1.10 to 1.01 as a function of La concentration. The trend is visualized using a line with an exponential fit on the measured data. The rhombohedral distortion varies with increasing La concentration between 0.0003 and 0.0042 without exhibiting any significant trend. For comparison, the rhombohedral and tetragonal distortions of PZT at MPB have been reported to lie at 0.007 and 1.022, respectively.<sup>24</sup> As the tetragonal distortion in BF-PT in the MPB region is much higher than the rhombohedral distortion, the tetragonal distortion is suggested to dominate the level of domain switching and piezoelectric properties of BF-PT.

The evolution of polarization and bipolar and unipolar strain hysteresis loops as a function of La concentration is presented in Figs. 2(a)–2(c). The shape of the polarization hysteresis loops [Fig. 2(a)] indicates that no noticeable change is induced in the domain configuration in BF-PT systems doped with less than 5 at % La. This is also evident from the very small strain response both in the bipolar and unipolar strain hysteresis loops [Figs. 2(b) and 2(c), respectively]. Even though these compositions do not show significant strain and polarization, they will still be considered as ferroelectric materials in this study, as they belong to a polar symmetry group. This is in accordance with literature<sup>9,10,20,25–27</sup> that reports on the existence of ferroelectric domains and domain reversal at extremely high fields even for low La content. When the concentration of La reaches 10 at %, there is a drastic enhancement both in

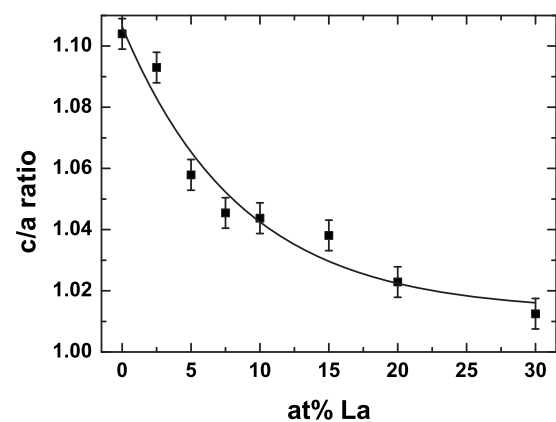


FIG. 1. Influence of La doping on tetragonal distortion of BF-PT.

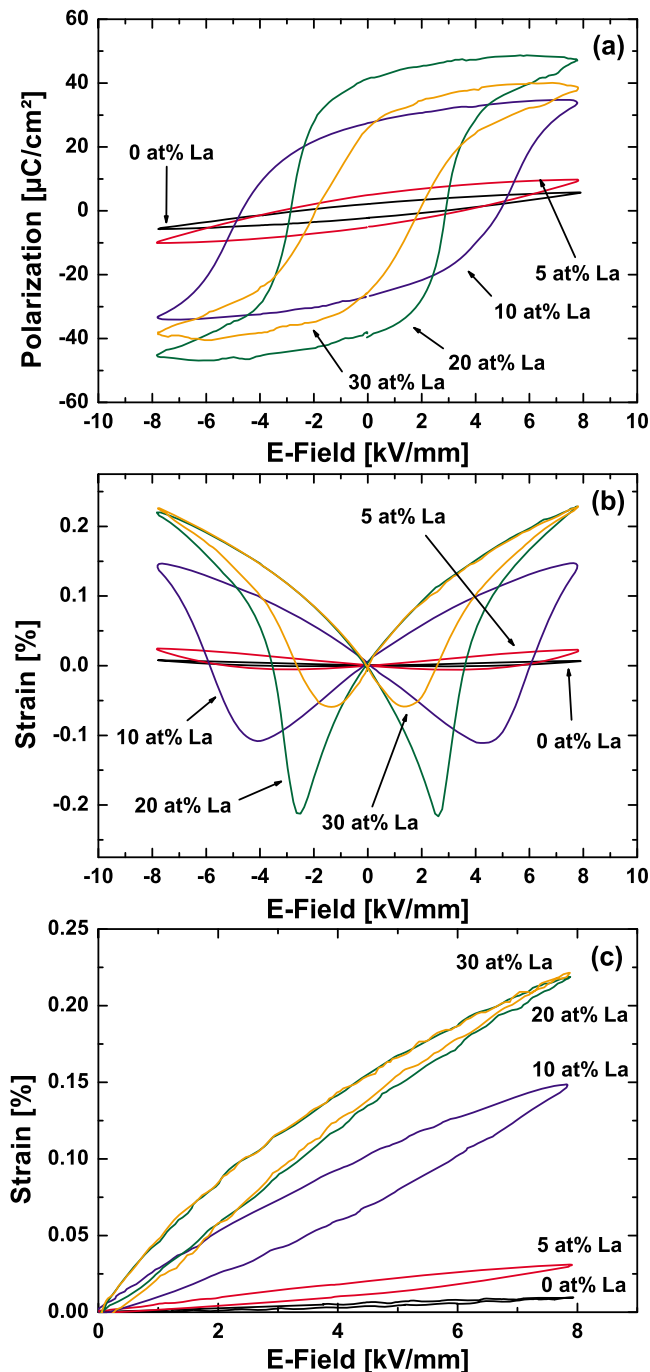


FIG. 2. (Color online) Electric field induced (a) polarization, (b) bipolar strain, and (c) unipolar strain hysteresis loops in La-doped BF-PT.

polarization and strain values. Note that the unipolar strain level of 10 at % La-doped BF-PT at 8 kV/mm is five times higher than that of 5 at % La-doped BF-PT, even though polarization and strain curves are not yet fully saturated. The shape of the loops is also observed to change. The polarization loops become more rectangular, and the strain loops evolve into a typical butterfly shape. At 30 at % lanthanum the polarization hysteresis loop becomes narrower and less steep at the coercive field, accompanied by a decrease in the negative strain, i.e., the difference between the minimum strain and the remanent strain in the bipolar strain hysteresis loop. Figures 3 and 4 display the remanent and maximum

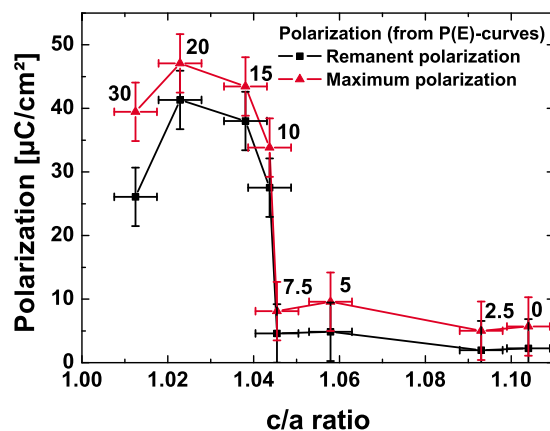


FIG. 3. (Color online) Effect of  $c/a$  ratio on the remanent and maximum polarization of La-doped BF-PT.

polarization values, and the total bipolar and unipolar strain levels, respectively, as a function of  $c/a$  ratio. The numbers next to the data markers refer to the corresponding La concentrations in atomic percent. Both the remanent and maximum polarization values increase sharply when the  $c/a$  ratio falls below 1.045 and then decrease notably at  $c/a=1.01$ . A similar tendency is also observed in the strain response as shown in Fig. 4. However, the unipolar strain keeps increasing even up to  $c/a=1.01$ . The small signal piezoelectric coefficient,  $d_{33}$ , as a function of  $c/a$  ratio was recorded after two unipolar poling cycles at 8 kV/mm (Fig. 5). It is seen that the  $c/a$  ratio affects the piezoelectric coefficient in a similar manner as it does polarization. The results of large-signal measurements may be affected by the particular maximum field chosen. Hence, complementary Rayleigh measurements were performed to evaluate reversible and irreversible domain wall motion at small alternating fields.<sup>28,29</sup> Figures 6(a) and 6(b) exemplarily display the dielectric permittivity,  $\epsilon_{33}$ , as a function of amplitude of the cycling field for samples doped with 0 and 20 at % La. For the undoped system the field dependent permittivity is linear only up to 600 V/mm and exhibits a decreasing slope for higher electric fields; a very similar behavior was found for the material doped with 2.5 at % La. This functional dependence is quite unusual, as  $\epsilon_{33}$  is expected to increase superlinearly when approaching the

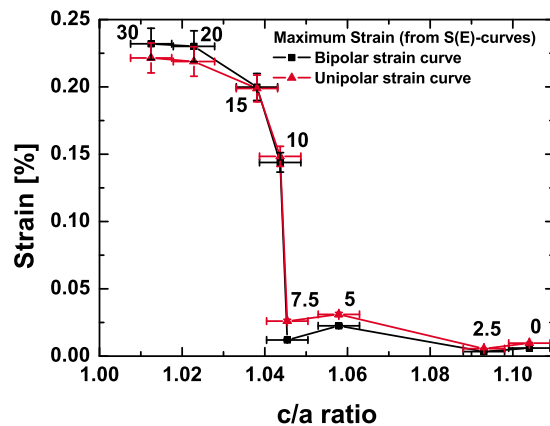
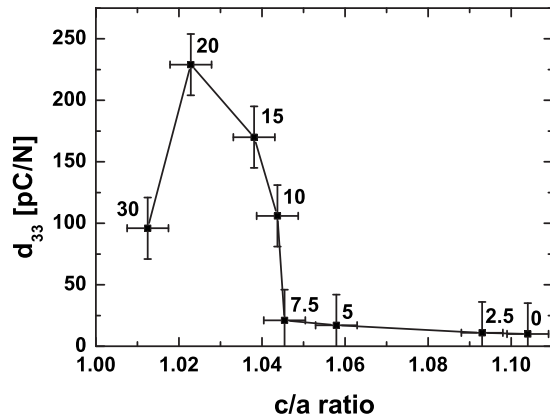


FIG. 4. (Color online) Effect of  $c/a$  ratio on bipolar and unipolar strain of La-doped BF-PT.

FIG. 5. Effect of  $c/a$  ratio on  $d_{33}$  of La-doped BF-PT.

high-field range of domain reversal in which domain nucleation takes place.<sup>30</sup> At 20 at % La the  $\epsilon(E)$ -graph is linear up to 800 V/mm, a behavior also found in a similar fashion in the materials doped with 5, 7.5, 10, and 30 at % La. The Rayleigh law allows investigation of domain wall behavior more closely, when fitting the linear portion of the permittivity with the following Eq. (1):<sup>30-33</sup>

$$\epsilon'_r(E_0) = \epsilon'_0 + \alpha'(E_0 - E'_t). \quad (1)$$

In this equation  $\epsilon'_r(E_0)$  is the dielectric permittivity at a given electric field  $E_0$ ,  $\epsilon'_0$  the zero field permittivity,  $\alpha'$  the Rayleigh coefficient, and  $E'_t$  the threshold field. The Rayleigh coefficient can be correlated with the irreversible domain wall motion induced by an external driving force, while the

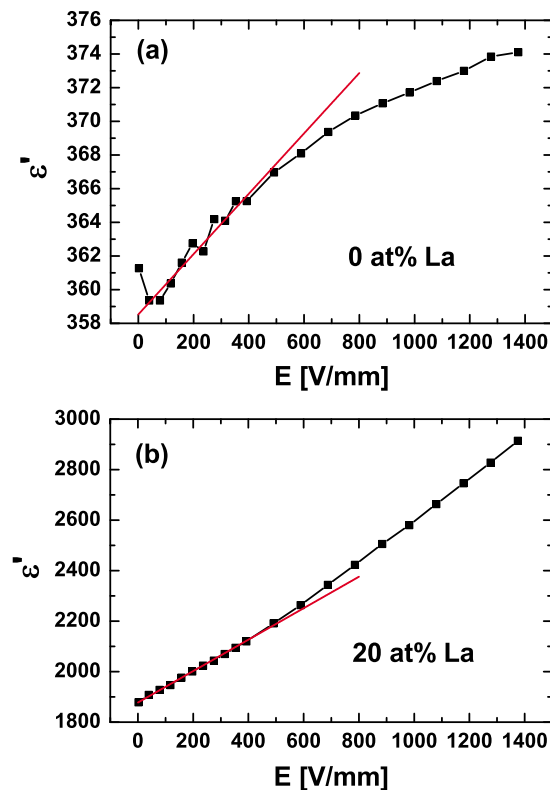
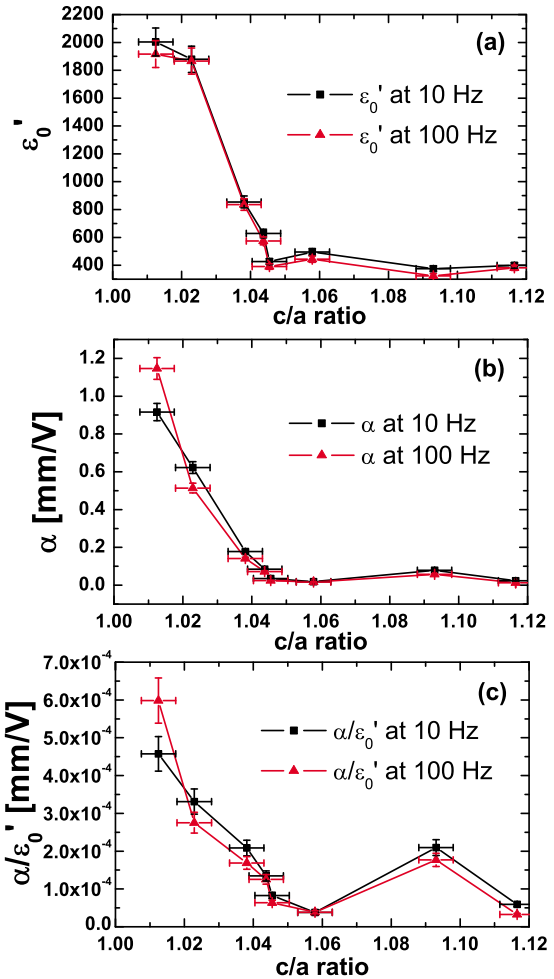


FIG. 6. (Color online) Dielectric permittivity as function of applied electric field for 0 at % (a) and 20 at % La (b). The line shows the linear fit with Eq. (1).

FIG. 7. (Color online) Zero field permittivity (a), Rayleigh parameter  $\alpha'$  (b), and the ratio between  $\alpha'$  and  $\epsilon'_0$  (c) as function of  $c/a$  ratio.

reversible domain wall vibration is connected to the zero field permittivity.<sup>30-33</sup> The calculated Rayleigh parameter  $\alpha'$  and the zero field permittivity are provided in Figs. 7(a) and 7(b) as a function of  $c/a$  ratio. Both parameters exhibit similar behavior. For high tetragonal distortions, there is no change in  $\alpha'$  and  $\epsilon'_0$  as a function of  $c/a$  ratio. In analogy to Figs. 3–5, a sharp increase in both Rayleigh values can be discerned for  $c/a$  ratios lower than 1.045. In contrast to the parameters investigated in Figs. 3–5, the increase is less steep, and  $\alpha'$  and  $\epsilon'_0$  keep increasing with decreasing  $c/a$  ratio.

#### IV. DISCUSSION

Internal compatibility stresses are shown to highly influence the switching behavior of ferroelectrics. These stresses can develop due to a phase transition from the paraelectric cubic phase into a tetragonal phase with a high  $c/a$  ratio.<sup>11,13</sup> If the stress level is high enough, it is possible to almost completely suppress domain switching.<sup>1</sup> In this regard, the hysteresis loops of the low-doped compositions presumably are a consequence of extremely suppressed domain switching. By increasing the La doping the internal stress level is decreased and thus, at a certain La concentration, the external field starts to induce a noticeable strain and polarization.

From Figs. 3–5 we conclude that there is a threshold value at a  $c/a$  ratio of about 1.045, above which domain switching is mostly suppressed. Also, nucleation of new domains is suppressed because of an increased elastic energy within the domain walls. Therefore, introducing new domain walls, e.g., by an electric field, is also difficult for high  $c/a$  ratios because it is energetically unfavorable. This also suggests that the number of domain walls is small for high  $c/a$  ratios and large for low  $c/a$  ratios. In  $(1-x)(\text{Bi}_{1-y}\text{La}_y)\text{FeO}_3-x\text{PbTiO}_3$  a change in domain wall density was reported by Li *et al.*<sup>34</sup> for  $x=0.55$ ,  $y=0.1$ ,  $0.2$ , and  $0.3$ , respectively, with increasing La concentration. The change of the  $c/a$  ratio is the only likely cause for the change in the electrical and electromechanical behavior. Other effects, such as the changes in grain size and density, are minor, and there seems to be no correlation between either of these parameters and the La content. However, it needs to be mentioned that the lowered Curie temperature might affect the value of the remanent polarization, especially for the 30 at % La doped composition.

For large-signal properties the above mentioned threshold value may depend on the specific field amplitude chosen (here 8 kV/mm) for the measurements. The Rayleigh measurements were utilized to draw conclusions on domain switching under small fields to determine if this threshold value is connected to the field amplitude, or if it is visible in the small-signal behavior as well. The total permittivity  $\epsilon$  is a combination of two contributing effects.<sup>35,36</sup> The first is the intrinsic effect caused by the deformation of the unit cell under an external electric field. The second is the extrinsic effect that is governed by domain wall mobility and the number of domain walls. It is unlikely that any change of the intrinsic contribution to the total dielectric permittivity is large enough to account for the drop in the permittivity by a factor of 5, expressed in the Rayleigh parameter  $\epsilon'_0$ , when the  $c/a$  ratio exceeds 1.045. This leaves a decrease in the number and the mobility of domain walls for high  $c/a$  ratios as possible explanations. It is suggested that both contribute to the low values of  $\epsilon'_0$  for low doping concentrations: in a highly distorted structure, the mismatch between domains with a different polarization orientation is high. The energy density stored in a domain wall is increased by the elastic mechanical deformation it has to accommodate. Therefore, the system will try to keep the number of domain walls as small as possible, resulting in a structure with large domains and few domain walls. This is corroborated by the fact that the slope of  $\epsilon'_r(E_0)$  decreases for high fields in the samples with low doping levels (0 and 2.5 at % La). Under normal conditions, nucleation of new domains would lead to a strong increase in  $\epsilon$ . As this is not observed, one can conclude that nucleation of new domains is largely suppressed. The decrease in the number of domain walls is not the only effect of the high  $c/a$  ratio.

As has been reported in several previous studies,<sup>30,31,33</sup> the parameter  $\alpha'$  can be correlated with irreversible domain wall motion. Therefore, the low value of  $\alpha'$  for  $c/a$  ratios above 1.045 indicates that there is only little irreversible domain wall motion present in the material. As described above for  $\epsilon'_0$ , this can again be due to a decrease in the domain wall

mobility or the number of domain walls. When the  $c/a$  ratio falls below 1.045,  $\alpha'$  increases, indicating an increase in irreversible domain wall motion due to the applied electric field. To quantify the influence of irreversible processes versus that of reversible processes, it is useful to look at the ratio  $\alpha'/\epsilon'_0$ ,<sup>28,29</sup> displayed in Fig. 7(c). It also decreases with increasing  $c/a$  ratio. This is a clear indication that the irreversible domain wall processes are impeded much more strongly than the reversible processes by a high tetragonal distortion. Irreversible domain wall processes increase sharply below a threshold value of 1.045. This threshold value, observed also in the large-signal hysteresis, does not depend on the cycling amplitude, as it is visible also in the small-signal parameters. Below the value of 1.045 the Rayleigh parameters increase not as strongly as the large- and small-signal parameters do and do not revert back at low tetragonal distortions.

There is a secondary effect related to the sample doped with 30 at % La. Polarization as well as piezoelectric coefficient decrease at very small  $c/a$  ratio, while strain shows no change. From Fig. 2(a), a wide distribution in local coercive fields can be deduced. We propose that this effect is partially due to the fact that the Curie temperature for this material is much closer to room temperature than that of the other samples (see Table I). It is possible that this temperature effect causes a destabilization of the domain structure induced by high external fields.

It has to be noted here that one should expect a logarithmic decrease in the Rayleigh parameters with increasing measurement frequency.<sup>36–38</sup> We only took data for two measurement frequencies and therefore are not able to validate or invalidate this prediction, but it has to be noted that the ratio of the values measured at both frequencies seems somewhat erratic. In this context it is important to note that true Rayleigh behavior requires a reduction in domain wall motion by pinning at randomly distributed pinning centers. This condition is probably not fulfilled in our material, the domain wall motion is hindered by internal stresses due to the large unit cell distortion, and at the same time the internal stress is one of the decisive factors in the formation of the domain structure in the first place; therefore, the cause of pinning and the domain structure are not independent. Since even non-Rayleigh type mechanisms can create Rayleigh-type behavior,<sup>37</sup> this does not influence the analysis of the development of both Rayleigh parameters with changing  $c/a$  ratio.

These findings have direct implications for the development of new piezoelectric materials. Best piezoceramic actuators are expected to be found with a tetragonal distortion between 1.01 and 1.04, while best piezoelectric sensors are predicted to have  $c/a$  ratios between 1.02 and 1.04.

## V. CONCLUSIONS

It was demonstrated that the switching behavior of BF-PT is highly influenced by  $c/a$  ratio. A threshold value of 1.045 for the  $c/a$  ratio was identified, above which almost no domain switching takes place. Below this threshold polarization, strain and piezoelectric coefficient increase drastically, while the Rayleigh parameters also display a strong increase.

Materials with optimized performance are predicted to lie in the range of 1.01–1.04 for piezoceramic actuators and between 1.02 and 1.04 for piezoceramic sensors, respectively.

## ACKNOWLEDGMENTS

This work was supported by the Deutsche Forschungsgemeinschaft (DFG) under Grant No. RO954/20-1. The authors would like to thank Jens Suffner for his support in performing the x-ray diffraction experiments and Emil Aulbach and Michael Weber for building the Rayleigh measurement equipment.

- <sup>1</sup>C. S. Lynch, *Acta Mater.* **44**, 4137 (1996).
- <sup>2</sup>A. B. Schäufele and K. H. Härdtl, *J. Am. Ceram. Soc.* **79**, 2637 (1996).
- <sup>3</sup>H. Cao and A. G. Evans, *J. Am. Ceram. Soc.* **76**, 890 (1993).
- <sup>4</sup>T. Granzow, T. Leist, A. B. Kounga, E. Aulbach, and J. Rödel, *Appl. Phys. Lett.* **91**, 142904 (2007).
- <sup>5</sup>B. S. Kwak, A. Erbil, J. D. Budai, M. F. Chrisholm, L. A. Boatner, and B. J. Wilkens, *Phys. Rev. B* **49**, 14865 (1994).
- <sup>6</sup>G. Catalan, A. Janssens, G. Rispens, S. Csiszar, O. Seeck, G. Rijnders, D. H. A. Blank, and B. Noheda, *Phys. Rev. Lett.* **96**, 127602 (2006).
- <sup>7</sup>A. B. Kounga, T. Granzow, E. Aulbach, M. Hinterstein, and J. Rödel, *J. Appl. Phys.* **104**, 024116 (2008).
- <sup>8</sup>B. Jaffe, W. R. Cook, and H. Jaffe, *Piezoelectric Ceramics* (Academic, New York, 1971).
- <sup>9</sup>T. P. Comyn, S. P. McBride, and A. J. Bell, *Mater. Lett.* **58**, 3844 (2004).
- <sup>10</sup>T. P. Comyn, T. Stevenson, and A. J. Bell, *J. Phys. IV* **128**, 13 (2005).
- <sup>11</sup>S. A. Fedulov, P. B. Ladyzhinskii, I. L. Pyatigorskaya, and Y. N. Venetsev, *Sov. Phys. Solid State* **6**, 375 (1964).
- <sup>12</sup>V. V. S. S. Sai Sunder, A. Halliyal, and A. M. Umarji, *J. Mater. Res.* **10**, 1301 (1995).
- <sup>13</sup>A. J. Bell, A. X. Levander, S. L. Turner, and T. P. Comyn, Proc. 16th IEEE ISAF, p. 406 (2007).
- <sup>14</sup>J. R. Cheng and L. E. Cross, *J. Appl. Phys.* **94**, 5188 (2003).
- <sup>15</sup>J. R. Cheng, R. Eitel, and L. E. Cross, *J. Am. Ceram. Soc.* **86**, 2111 (2003).
- <sup>16</sup>J. R. Cheng and L. E. Cross, *IEEE Ultrasonics Symposium*, **1**, 354 (2003).
- <sup>17</sup>J. Cheng, S. Yu, J. Chen, Z. Meng, and L. E. Cross, *Appl. Phys. Lett.* **89**, 122911 (2006).
- <sup>18</sup>Y. Hadas, A. Sayapin, Y. E. Krasik, V. Bernshtam, and I. Schnitzer, *J. Appl. Phys.* **104**, 064125 (2008).
- <sup>19</sup>T. Leist, W. Jo, T. Comyn, A. Bell, and J. Rödel, *Jpn. J. Appl. Phys.* **48**, 120205 (2009).
- <sup>20</sup>D. I. Woodward and I. M. Reaney, *J. Appl. Phys.* **94**, 3313 (2003).
- <sup>21</sup>A. C. Larson and R. B. Von Dreele, Los Alamos National Laboratory Report No. LAUR 86, 2000.
- <sup>22</sup>B. H. Toby, *J. Appl. Crystallogr.* **34**, 210 (2001).
- <sup>23</sup>N. Uchida and T. Ikeda, *Jpn. J. Appl. Phys.* **6**, 1079 (1967).
- <sup>24</sup>H. Kungl, R. Theissmann, M. Knapp, C. Baehtz, H. Fuess, S. Wagner, T. Fett, and M. J. Hoffmann, *Acta Mater.* **55**, 1849 (2007).
- <sup>25</sup>T. L. Burnett, T. P. Comyn, and A. J. Bell, *J. Cryst. Growth* **285**, 156 (2005).
- <sup>26</sup>M. A. Khan, T. P. Comyn, and A. J. Bell, *Appl. Phys. Lett.* **91**, 032901 (2007).
- <sup>27</sup>M. A. Khan, T. P. Comyn, and A. J. Bell, *Acta Mater.* **56**, 2110 (2008).
- <sup>28</sup>N. B. Gharb and S. Trolier-McKinstry, *J. Appl. Phys.* **97**, 064106 (2005).
- <sup>29</sup>N. Bassiri-Gharb, I. Fujii, E. Hong, S. Trolier-McKinstry, D. V. Taylor, and D. Damjanovic, *J. Electroceram.* **19**, 49 (2007).
- <sup>30</sup>D. A. Hall and P. J. Stevenson, *Ferroelectrics* **228**, 139 (1999).
- <sup>31</sup>D. Damjanovic and M. Demartin, *J. Phys. D: Appl. Phys.* **29**, 2057 (1996).
- <sup>32</sup>D. Damjanovic and M. Demartin, *J. Phys.: Condens. Matter* **9**, 4943 (1997).
- <sup>33</sup>D. A. Hall, *Ferroelectrics* **223**, 319 (1999).
- <sup>34</sup>Z. A. Li, H. X. Yang, H. F. Tian, and J. Q. Li, *Appl. Phys. Lett.* **90**, 182904 (2007).
- <sup>35</sup>R. Herbiet, U. Robels, H. Dederichs, and G. Arlt, *Ferroelectrics* **98**, 107 (1989).
- <sup>36</sup>D. A. Hall, *J. Mater. Sci.* **36**, 4575 (2001).
- <sup>37</sup>D. Damjanovic, *J. Appl. Phys.* **82**, 1788 (1997).
- <sup>38</sup>D. V. Taylor and D. Damjanovic, *J. Appl. Phys.* **82**, 1973 (1997).